AKADÉMIAI KIADÓ

UNIVERSITY of DEBRECEN

International Review of Applied Sciences and Engineering

15 (2024) 3, 355–364

DOI:
10.1556/1848.2024.00789


ORIGINAL RESEARCH PAPER



# Electrical faults classification in permanent magnet synchronous motor using ResNet neural network

Hiba Ziad[1], Ayad Al-dujaili[1]* and Amjad J. Humaidi[2]

[1] Electrical Engineering Technical College, Middle Technical University, Baghdad, Iraq

[2] Control and Systems Engineering Department, University of Technology, Baghdad, Iraq

Received: December 21, 2023 • Accepted: February 22, 2024
Published online: April 9, 2024

**ABSTRACT**

The predictive maintenance of permeant magnet synchronous motor is highly required as this kind of motor has been commonly employed in electric vehicles, industrial systems, and other applications owing to its high power density output, as well as the regenerative operation characteristics during braking and deceleration driving conditions. One of the most important causes of PMSM failure is the stator short and drive switches failure. These problems have attracted more attention in the field of deep learning for fault detection purposes in the early stages, to avoid any system breakdown, and to decrease the risk and price of maintenance. In this paper, we investigate the possibility of detecting the electrical faults in PMSM by generating our data which includes current signals that have been analyzed and preprocessed by applying Continuous Wavelet Transform (CWT) to select the reliable features this conversion will be used to train ResNet 50. The evaluation metrics have shown that ResNet 50 achieves an accuracy of 100% for the classification of faults.

**KEYWORDS**

PMSM, ResNet, CWT, fault classification

## 1. INTRODUCTION

PMSMs are a type of motor that exhibits superior dynamic performance and exceptional dependability. Because PMSM motors are utilized to drive a range of loads, they are an invaluable tool in the transportation, aerospace, and industrial automation sectors. Because the permanent magnet synchronous motor does not require slip rings for field excitation, it requires less maintenance and has lower rotor losses. Because of their great efficiency, PMSMs are suitable for high-performance drive systems found in the industry, for instance CNC machines and robotic and autonomous production systems [1]. There are three types of failures in PMSMs: mechanical, electrical, and magnetic. The creation and dispersion of magnetic field lines are connected to magnetic faults. Stator faults and external problems (connected to drives) are two other categories of electrical defects. The majority of insulation-based failures occur in the winding section of the stator. Typically, insulation failure is the cause of these defects. Fault prediction in PMSMs is required to improve their performance, lengthen their lifespan, and reduce their expensive costs [2].

Electric motor fault recognition and evaluation have been thoroughly studied to date such as the method that depends on knowledge, signal, model, and combinations of these methods. A model-based system requires a precise computational model, on the other hand, a signal-based system is highly reliant on the operation point of the machine [3, 4]. Conversely, knowledge-based categorization arranges the fault types using a large number of experimental datasets. Therefore, data-driven approaches are appropriate for specific signal sequences or highly nonlinear structures with an unknown model [5]. The idea is basically to

*Corresponding author.
E-mail: ayad.qasim@mtu.edu.iq

AKJournals

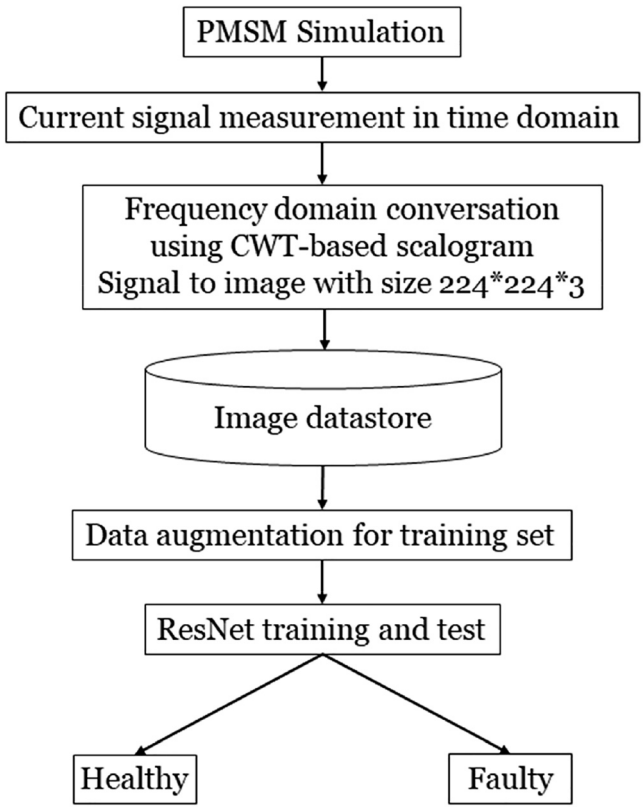


*Fig. 1.* Process for diagnosing faults

train the Deep Learning Network with data from both healthy and malfunctioning motors to eventually distinguish between the two and have the capacity to warn when a motor is about to break down before it happens.

In the last decade, Artificial Intelligence has been wildly developed and has been employed for fault detection in electrical motors. In the past few years, a lot of researchers paid attention to the detection and classification of PMSM fault by employing machine learning (ML) techniques such as the k-nearest neighbor (KNN) algorithm [6], generative adversarial networks [7], support vector machines (SVM) [8], artificial neural networks [9], and linear regression [10].

Abed et al. [10] used the Multilayer Perceptron (MLP) feed-forward neural network to classify the inter-turn short circuit issue in the PMSM stator winding. In [11], Chen et al. created the Autoregressive of the Nonlinear Utilizing Exogenous Model (NARX), a series of techniques controlled to determine the degree of fault in an open circuit emerging through a toggle switch in aircraft PMSM.

Over the past 20 years, deep learning (DL) has been shown to be an extremely effective method for fault prediction in a variety of industries [12–16], showcasing its capacity to automatically recognize characteristics from raw data. As a result, it can reduce reliance on human experts' diagnostic expertise (meaningful feature extraction and selection). Furthermore, by employing a multilayer design, DL can establish a connection between the type of failure and the experimental data. Numerous deep learning (DL) approaches, including convolution neural networks (CNN) [17] and deep belief networks (DBNs) [18], have already been employed for fault identification. CNN is widely used in defect identification due to its capacity to extract meaningful hierarchical features [17]. The time-domain signals are the most widely accessible data. Moreover, the development of a massive number of defective machine data is laborious in the FDI sector, and DL approaches rely on a substantial amount of data to maximize the category masses

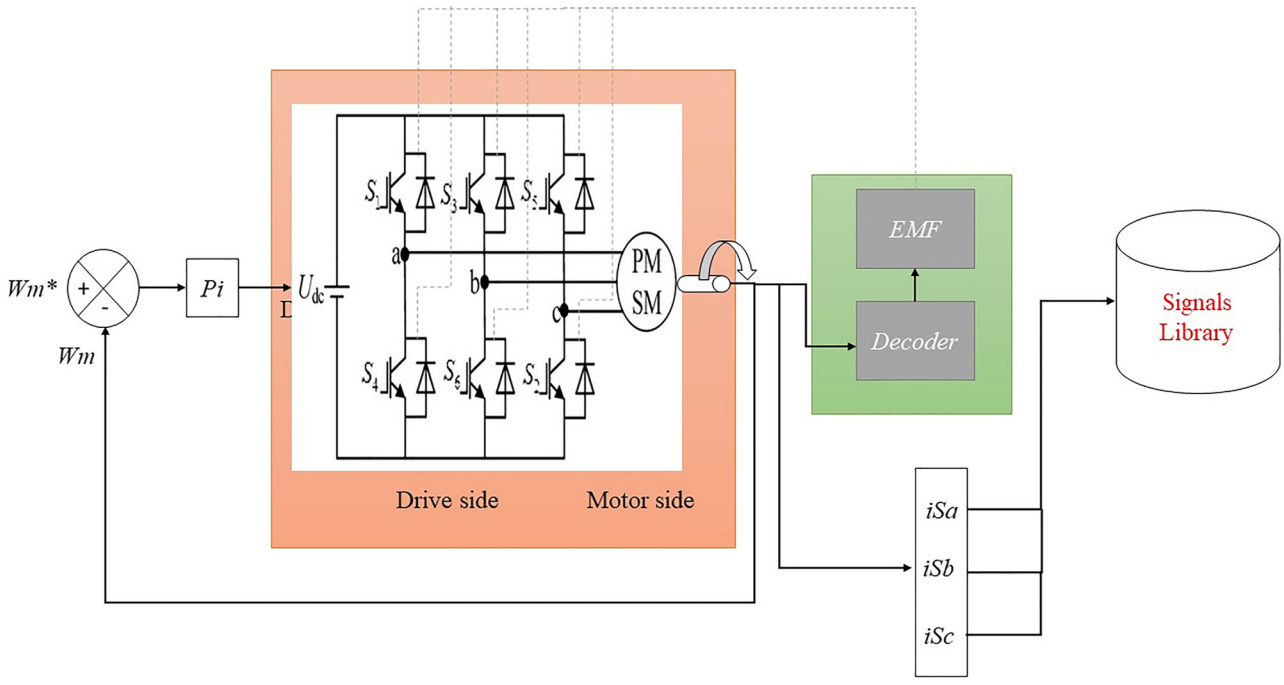


*Fig. 2.* Simulation of PMSM and signal collection

for predictions. Furthermore, when dealing with limited datasets that have a higher number of trainable issues, deep learning networks also tend to overfit. Hence, before being used in the FDI area, DL techniques require special architectural enhancements.

The motor data generated and labeled manually from the simulation is limited and contains a variation in the period domain especially in faulty cases. The raw signal in time series of the stator current is converted to the time-frequency domain via employing continuous wavelet transform (CWT) which allows the extraction of reliable features simply without losing any information in the original signal. These limitations inspired us to investigate the residual network (ResNet) ability to classify the sudden changes in the frequency when a malfunction occurs without using transfer learning and to study the impact of training factors on the category results such as batch size, learning rate, and data division. This will reduce the probability of the model to be overfitted.

This research aims to develop a classification method for PMSM stator current where the measured stator current does not require monitor devices or complicated signal proceeding techniques. Furthermore, the CWT-based scalogram can extract high-order features from the original signal that will improve the accuracy percentage of the classification system. Also, the use of ResNet has reduced the need for human intervention and expertise in feature extraction and selection.

The paper is arranged into five sections. The introduction which is presented in the first section followed by the second section which presents the principle of proposed work that starts with the simulation of PMSM and faults generation, data acquisition and transformation, data augmentation, and ends with the training of the ResNet structure. In the third section, the experimental results are presented in details and it is followed by discussion in the fourth section. Finally, the summary of the proposed method and the future work are introduced in section five.

*Table 1.* Three-phase PMSM mechanical and electrical parameters

| Parameter | Value | Unit |
|---|---|---|
| The resistance of stator, *Rs* | 2.8 | Ω |
| Leakage inductance of stator, *Lis* | 0.42 | H |
| Flux linkage, λ | 0.175 | Wb |
| Rated speed, *Wm* | 3,000 | RPM |
| Moment of inertia, *J* | 0.03 | $Kg.m^2$ |
| No. of poles | 3 | – |

## 2. FAULT CLASSIFICATION METHOD

The experiment is completely based on diagnosing faults in a PMSM under various operating scenarios using frequency-

*Table 2.* Lookup table of the fault generated from the inverter side

| Fault type | Phase | S1 | S2 | S3 | S4 | S5 | S6 |
|---|---|---|---|---|---|---|---|
| Open circuit | 'A' | OFF | ON | ON | ON | ON | ON |
| | 'A' | ON | ON | ON | OFF | ON | ON |
| | 'B' | ON | ON | OFF | ON | ON | ON |
| | 'B' | ON | ON | ON | ON | ON | OFF |
| | 'C' | ON | ON | ON | ON | OFF | ON |
| | 'C' | ON | OFF | ON | ON | ON | ON |
| | 'A', 'C' | OFF | OFF | ON | ON | ON | ON |
| | 'A', 'B' | OFF | ON | ON | ON | ON | OFF |
| | 'A', 'B' | ON | ON | OFF | OFF | ON | ON |
| | 'B', 'C' | ON | OFF | OFF | ON | ON | ON |
| | 'A', 'C' | ON | ON | ON | OFF | OFF | ON |
| | 'B', 'C' | ON | ON | ON | ON | OFF | OFF |
| | 'A', 'B' | OFF | ON | OFF | ON | ON | ON |
| | 'B, 'C' | ON | ON | OFF | ON | OFF | ON |
| | 'A', 'C' | OFF | ON | ON | ON | OFF | ON |
| | 'A', 'C' | ON | ON | ON | OFF | ON | OFF |
| | 'B', 'C' | ON | OFF | ON | ON | ON | OFF |
| | 'A', 'B' | ON | OFF | ON | OFF | ON | ON |
| | 'A', 'B', 'C' | OFF | ON | OFF | ON | OFF | ON |
| | 'A', 'B', 'C' | ON | OFF | ON | OFF | ON | OFF |
| | 'A', 'B', 'C' | OFF | ON | ON | ON | OFF | OFF |
| | 'A', 'B', 'C' | ON | OFF | OFF | OFF | ON | ON |
| | 'A', 'B', 'C' | OFF | OFF | ON | OFF | ON | OFF |
| | 'A', 'B', 'C' | ON | OFF | OFF | OFF | ON | OFF |
| | 'A', 'B', 'C' | ON | OFF | ON | OFF | OFF | OFF |
| | 'A', 'B', 'C' | OFF | ON | OFF | OFF | OFF | ON |
| | 'A', 'B', 'C' | OFF | ON | OFF | ON | OFF | OFF |
| | 'A', 'B', 'C' | OFF | OFF | OFF | ON | OFF | ON |

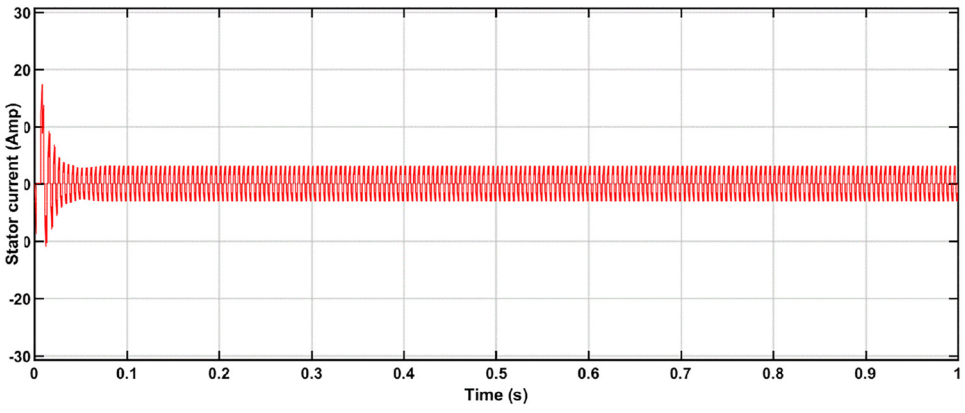


*Fig. 3.* Represents the phase 'B' current signal under normal operation

domain properties. When the motor operates under various conditions, the fundamental frequency of the stator current varies, resulting in a variation in the fault frequency. As this study focuses on the classification of electrical faults which includes driving failures and stator winding short-turn faults are frequent; the most obvious kind is inter-turn short-circuit. Electrical malfunctions can generally be classified as connection errors, ground errors, stator phase winding short circuits, and full phase open circuits. The most prevalent of those defects is known as the Inter-Turn Short Fault (ITSF), and this research will primarily examine it. At each simulation, the measured current signal will be processed by applying CWT and converted to an image that carries the best features in the original signal. After establishing the faulty and healthy feature library, three types of ResNet networks will be trained for classification purposes as shown in Fig. 1.

## 2.1. PMSM Simulink model and data acquisition

The characteristics of permanent magnet synchronous motor include current, voltage, torque, magnetic flux, and vibration, can vary due to any type of defect. However, the information carried by the phase current signal is more useful. As seen in "Fig. 2" which demonstrates the PMSM simulation model used to gather phase current signals through the use of the Sim Power system toolbox in the Matlab/Simulink environment. To provide an AC output with a changeable frequency, the inverter modifies the input DC voltage. In PMSM there are two modes of operation, generator or motor, and this can be done by the mechanical torque's 'T' sign (negative sign for generator mode, positive sign for motor mode). It is possible to modify the speed in a closed loop through determining the real rotor speed and comparing it to the reference speed. The inputs to the PMSM block are the three-phase inverter, load torque, and terminal phase voltages.

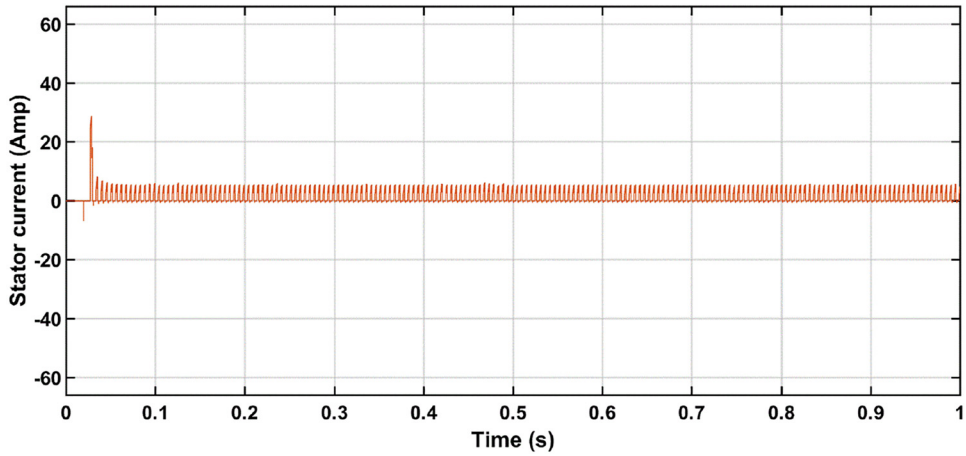


*Fig. 4.* Illustrates the phase 'B' current signal under abnormal operation

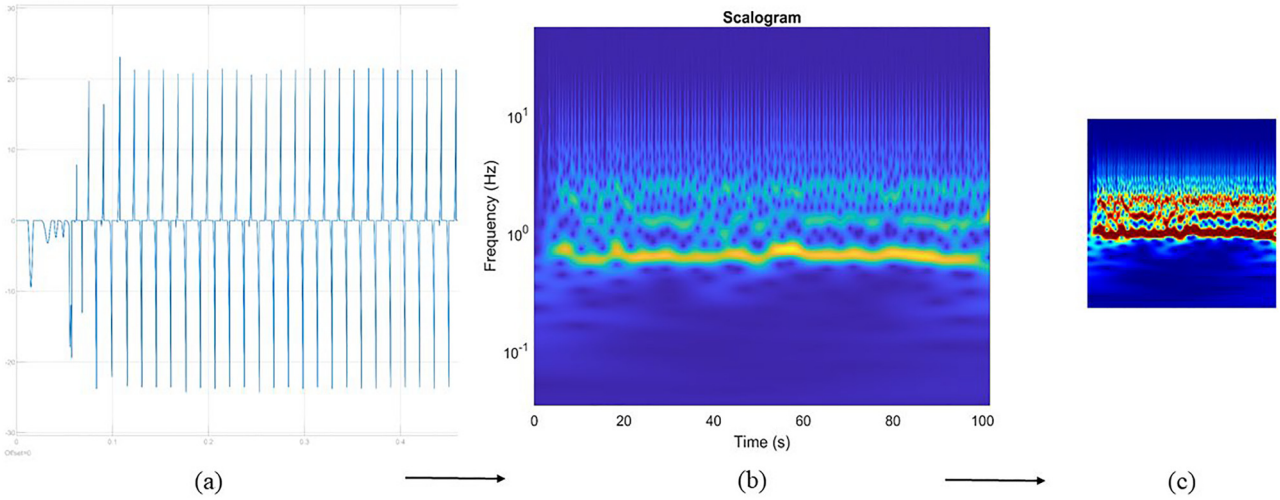


*Fig. 5.* Demonstrate data processing where (a) represents the raw data (time-domain signal), (b) the scalogram image obtained from the absolute value of the CWT, and (c) illustrates the final image which is 2D image of size 224*224*3

To generate our data, the PMSM was experimentally tested under standard operation. The specification of the motor is described in Table 1. The stable speed of the motor indicates that the motor is running under normal operation, and that the current phase signal has no sudden changes in the amplitude. The experimental model shown in Fig. 2 was composed of a three-phase PMSM fed by a leg inverter supplied by a DC voltage source 500 V. The phase of 'B' measured current signal is represented in Fig. 3 as a sample of time series current signal of the motor under healthy operation.

Now to introduce the fault signals, the PMSM was emulated in different scenarios and a lookup table (see Table 2) was made to introduce both open and short circuit faults for the drive side. For motor faults, coil-coil fault and coil-to-ground fault have been added and the fault was injected during the simulation after 0.2 s of operation. The fault resistance value was set to a minimum till the sudden change occurred in the phase current signal.

Additionally, open circuit faults in a single or multiple phase can be achieved by removing the IGBT of phase leg 'X' before motor simulation and the same steps were repeated for multiple phases of open circuit fault as described in Table 2, and illustrated in Fig. 4 as sample of time series of the measured current signal when the motor operated under unhealthy condition. However, to generate a phase short circuit, we repeated the same lookup table but in this case, we manipulated several IGBT parameters for the leg phase such as the internal resistance, the forward voltage of the IGBT device, the snubber resistance (this was set to minimum or eliminated), and the snubber capacitance.

## 2.2. Data transformation and augmentation

The phase current signal in the time domain was gathered and analyzed at various lengths that can be transformed into the frequency domain using the continuous wavelet transform (CWT), which uses the inner products to calculate the similarity of a signal to the function of analysis. A simple illustration of this idea is shown in Fig. 5.

The absolute value of the CWT is called the scalogram image and it can be obtained from the time scale spectrum and amplitude produced by the CWT. Then, the 2D image can be achieved by recalculating the filter bank number which depends on the length of the time series signal [18].

There are 526 labels in the dataset, one for every class. Even when the dataset already has extracted characteristics, pretreatment is still necessary to prevent overfitting and to greatly enhance the efficiency of deep learning models during training. However, the system behaves subparly when detecting the minority class due to bias across the presiding class. To prevent that, data balancing is carried out. Additionally, a modified version of the original dataset has been added to the quantity through the use of methods for data enhancement. On the training dataset alone, we used five different kinds of data augmentation techniques, including random rotation, vertical cropping, horizontal cropping, and reflection as techniques contributing to raising the accuracy of the model, in addition to the random chosen of the training dataset at each epoch.

## 2.3. Training setup

In the present research, a $224 \times 224$ pre-processed RGB image is fed into the neural network, which divides it into two classes: Healthy and Faulty. Since the suggested ImageNet-based pre-trained ResNet model was applied, our data had to be utilized to develop the dense and dropout levels of the classification layers from scratch. However, the convolution layer of the ResNet model was run on our training dataset, generating the final layer output vectors. The Soft max classifier is used as a classification layer which will train on the output vectors of the final layer. The experiment is implemented by using a Matlab environment with a single CPU. The training dataset was randomly chosen from the original dataset at

*Table 3.* Results of ResNet 18

| Network | Data Div. | Mini batch | Learn rate | Metrics | | | |
|---|---|---|---|---|---|---|---|
| | | | | ACC | F1 | Recall | Precision |
| ResNet 18 | 60% | 32 | 0.1 | 82.9 | 79.4 | 100 | 65.9 |
| | | | 0.01 | 78.7 | 74.3 | 93.5 | 61.7 |
| | | | 0.001 | 95.7 | 95.6 | 94.6 | 96.7 |
| | | | 0.0001 | 96.3 | 96.1 | 100 | 92.5 |
| | | 16 | 0.1 | 75.5 | 67.6 | 100 | 51 |
| | | | 0.01 | 92 | 91.8 | 93.4 | 90.4 |
| | | | 0.001 | 94.1 | 93.8 | 98.8 | 89.3 |
| | | | 0.0001 | 95.7 | 95.6 | 97.7 | 93.6 |
| | | 8 | 0.1 | 83 | 81.8 | 87.8 | 76.5 |
| | | | 0.01 | 95.7 | 95.6 | 97.7 | 93.6 |
| | | | 0.001 | 91.4 | 94.2 | 88.2 | 94.3 |
| | | | 0.0001 | 91.5 | 91.8 | 88.2 | 95.7 |
| | 70% | 32 | 0.1 | 77.5 | 70.9 | 100 | 54.9 |
| | | | 0.01 | 88.7 | 87.3 | 100 | 77.4 |
| | | | 0.001 | 97.2 | 97.1 | 98.5 | 95.7 |
| | | | 0.0001 | 99.3 | 99.2 | 100 | 98.5 |
| | | 16 | 0.1 | 88 | 87.4 | 92.1 | 83 |
| | | | 0.01 | 93.7 | 93.3 | 98.4 | 88.7 |
| | | | 0.001 | 93.7 | 93.7 | 93 | 94.3 |
| | | | 0.0001 | 95.1 | 95.3 | 91.1 | 100 |
| | | 8 | 0.1 | 80.3 | 76.2 | 95.7 | 63.3 |
| | | | 0.01 | 93 | 92.6 | 96.9 | 88.7 |
| | | | 0.001 | 95.1 | 94.8 | 100 | 90.1 |
| | | | 0.0001 | 95.1 | 94.8 | 100 | 90.1 |
| | 80% | 32 | 0.1 | 83 | 83.6 | 80.3 | 87.2 |
| | | | 0.01 | 93.6 | 93.1 | 100 | 87.2 |
| | | | 0.001 | 97.8 | 97.8 | 100 | 95.7 |
| | | | 0.0001 | 97.8 | 97.8 | 97.8 | 97.8 |
| | | 16 | 0.1 | 79.8 | 75.3 | 96.6 | 61.7 |
| | | | 0.01 | 90.4 | 89.4 | 100 | 80.8 |
| | | | 0.001 | 90.4 | 91.2 | 83.9 | 100 |
| | | | 0.0001 | 98.9 | 98.9 | 100 | 97.8 |
| | | 8 | 0.1 | 50 | 0 | 0 | 0 |
| | | | 0.01 | 90.4 | 89.4 | 100 | 80.8 |
| | | | 0.001 | 96.8 | 96.8 | 95.8 | 97.8 |
| | | | 0.0001 | 98.9 | 98.9 | 100 | 97.8 |

each training process and the division of training data was started with 60%, 70%, and 80% respectively. The number of epochs was set as 10. The Adaptive Moment Estimation (Adam) algorithm was used and the learning rate was used as 0.1, 0.01, 0.01, 0.001, and 0.0001 respectively. The batch size during training was started as 32, 16, and 8, respectively.

## 3. EXPERIMENTAL RESULTS

To reflect the general efficacy of a classification model when examined on a set of test data, the confusion matrix is used to combine the true positive, true negative, false positive, and false negative in one table for each labelled class. Confusion matrix is built by comparing the observed class labels in the test dataset to the predicted class labels given by the model. Rows indicate the actual class labels, whereas columns show the expected class labels. However, the experiment results of the proposed method were evaluated by checking the variations between the real categories and the classifications produced by the classifier, and this process is called the accuracy which can be calculated as follows:

$$ACC = \frac{TP + TN}{TP + TN + FN + FP} \quad (1)$$

where true positive refers to the model which correctly predicted the positive cases and it is symbolized by TP. Correspondingly, true negative refers to the model that correctly identified negative cases and it is denoted by TN. Additionally, the false positive represents wrong model's prediction number of positive classes and it is denoted by FP, while the FN refers to the model which incorrectly predicted the negative cases. Furthermore, the Recall metric evaluates how well the model can detect every positive case. It can be computed by dividing the total number of actual positive forecasts using the number of true positive predictions produced by the model:

$$Recall = \frac{TP}{TP + FN} \quad (2)$$

The ratio of TP forecasts to all positive predictions is called precision which evaluates the model's potential to identify affirmative cases and it can be calculated as follows:

$$Precision = \frac{TP}{TP + FP} \quad (3)$$

Last but not least, the system's ability to balance the harmonic mean of precision and recall is called the F1 score and it can be calculated as follows:

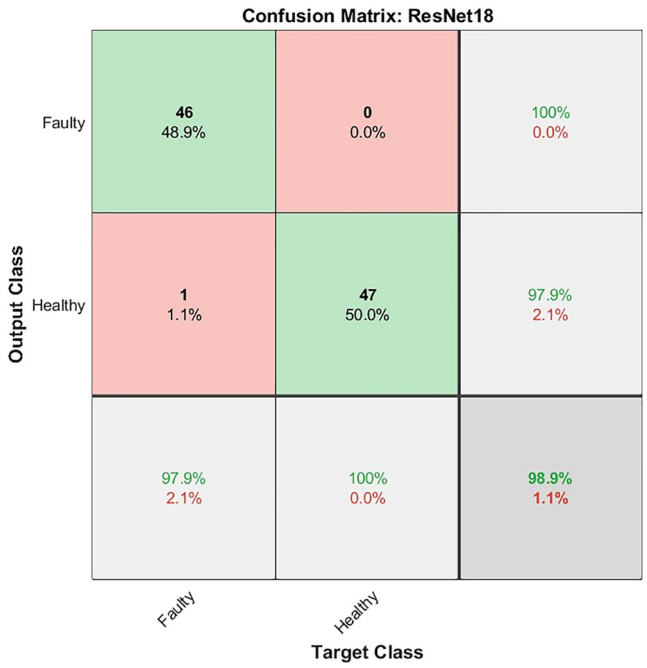


*Fig. 6.* Confusion matrix of ResNet 18

*Table 4.* Results of ResNet 50

| Network | Data Div. | Mini batch | Learn rate | Metrics | | | |
|---|---|---|---|---|---|---|---|
| | | | | ACC | F1 | Recall | Precision |
| ResNet 50 | 60% | 32 | 0.1 | 75.5 | 67.6 | 100 | 51 |
| | | | 0.01 | 88.8 | 87.4 | 100 | 77 |
| | | | 0.001 | 93.6 | 93.4 | 95.5 | 91.4 |
| | | | 0.0001 | 97.3 | 97.2 | 100 | 94.6 |
| | | 16 | 0.1 | 74.4 | 66.6 | 96 | 51 |
| | | | 0.01 | 81.3 | 77.9 | 95.3 | 65.9 |
| | | | 0.001 | 93.6 | 96.7 | 96.5 | 90.4 |
| | | | 0.0001 | 97.3 | 97.3 | 97.8 | 96.8 |
| | | 8 | 0.1 | 57.3 | 80.7 | 93 | 71.2 |
| | | | 0.01 | 78.1 | 73.2 | 94.9 | 59.5 |
| | | | 0.001 | 83.5 | 85.4 | 76.4 | 96.8 |
| | | | 0.0001 | 93.6 | 93.3 | 97.6 | 89.3 |
| | 70% | 32 | 0.1 | 66.2 | 48.9 | 100 | 32.3 |
| | | | 0.01 | 76 | 69 | 97.4 | 53.5 |
| | | | 0.001 | 94.3 | 94.4 | 93.1 | 95.7 |
| | | | 0.0001 | 98.5 | 98.5 | 100 | 97.1 |
| | | 16 | 0.1 | 76.7 | 69.7 | 100 | 53.5 |
| | | | 0.01 | 81.6 | 77.9 | 97.8 | 64.7 |
| | | | 0.001 | 92.9 | 93.1 | 90.6 | 95.7 |
| | | | 0.0001 | 94.4 | 94 | 100 | 88.7 |
| | | 8 | 0.1 | 77.5 | 79.7 | 72.4 | 88.7 |
| | | | 0.01 | 67.6 | 52 | 100 | 35.2 |
| | | | 0.001 | 88 | 86.4 | 100 | 76 |
| | | | 0.0001 | 94.4 | 94 | 100 | 100 |
| | 80% | 32 | 0.1 | 71.3 | 59.7 | 100 | 42.5 |
| | | | 0.01 | 78.7 | 78.7 | 78.7 | 78.7 |
| | | | 0.001 | 95.7 | 95.6 | 97.7 | 93.6 |
| | | | 0.0001 | 98.9 | 98.9 | 100 | 97.8 |
| | | 16 | 0.1 | 78.7 | 73.6 | 96.5 | 59.5 |
| | | | 0.01 | 81.9 | 79 | 94.1 | 68 |
| | | | 0.001 | 94.6 | 94.3 | 100 | 89.3 |
| | | | 0.0001 | 98.9 | 98.9 | 100 | 97.8 |
| | | 8 | 0.1 | 50 | 66 | 50 | 100 |
| | | | 0.01 | 83 | 80 | 96.9 | 68 |
| | | | 0.001 | 93.6 | 93.4 | 95.5 | 91.4 |
| | | | 0.0001 | 100 | 100 | 100 | 100 |

$$F1\ Score = \frac{2 * TP}{2 * TP + FN + FP} \quad (4)$$

The experimental results shows that the ResNet 18, which has a lowest number of layers compared to other models can classify both faulty and healthy images when trained with 80% of training dataset, and setting the batch size to 16, and learning rate 0.0001. It achieves accuracy of 98.9% as shown in Table 3, which represents the number of attempts to get the best classification performance that is presented in Fig. 6.

Furthermore, the experimental results of ResNet 50 shows that this model achieves accuracy of 100% when trained with 80% of training dataset, and setting the batch size to 8, and learning rate 0.0001 as shown in Table 4, which introduced the number of attempts to get the best classification performance and that is illustrated in Fig. 7.

For ResNet 101, the experimental results shows that this model achieves accuracy of 98.6% when trained with 70% of training dataset, and setting the batch size to 16, and learning rate 0.0001 as shown in Table 5 which introduced the number of attempts to get the best classification performance and that is illustrated in Fig. 8.

## 4. DISCUSSION

The assessed models generally had good accuracy, ranging from 93.6 to 100%. All models reached values greater than 93% in the recall ratings, which were likewise quite high. The confusion matrices in Figs 5–7 show that ResNet 50 behaves better than other structures even when trained with a low data limit, and it can detect sudden changes in faulty signals. Moreover, it achieves the best accuracy of 100% when trained with 80% of the training dataset, setting the batch size to 8, and the learning rate to 0.0001. This tuning improves the results of ResNet 50 which can be observed in accuracy, recall, precision, and F1 score as shown in Table 6. From the results of recall and precision, it can be noticed that both ResNet 18 and ResNet 101 have been overfitted, so they misclassified some malfunctions cases.

The results of ResNet 50 cast a new light on the possibility of employing this network for online electrical fault detection. It facilitates remote monitoring of the motor performance with the ability to predict the type of malfunction and to take appropriate action before it occurs. However, it is very possible to reduce the risks that may affect the motor, which may cause a certain production line to stop, or to avoid damage to other parts.

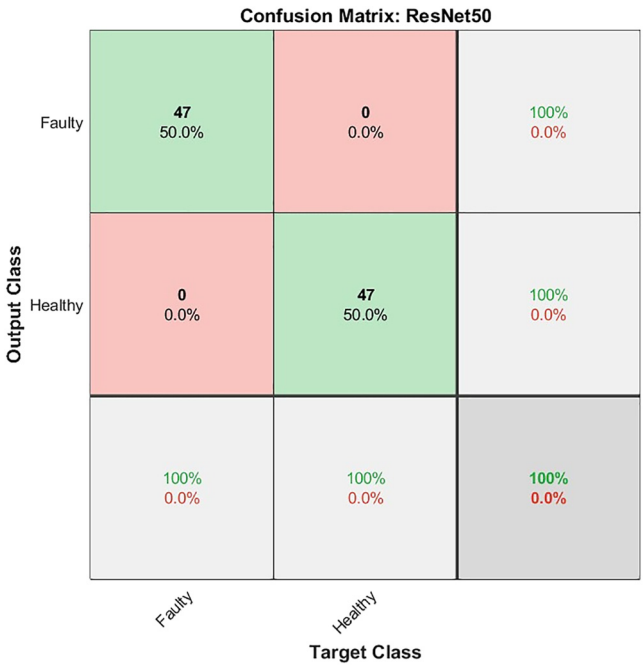


*Fig. 7.* Confusion matrix of ResNet 50

*Table 5.* Results of ResNet 101

| Network | Data Div. | Mini batch | Learn rate | Metrics | | | |
|---|---|---|---|---|---|---|---|
| | | | | ACC | F1 | Recall | Precision |
| ResNet 101 | 60% | 32 | 0.1 | 77.7 | 72 | 96.4 | 57.4 |
| | | | 0.01 | 66 | 51.1 | 89.4 | 36.1 |
| | | | 0.001 | 89.9 | 90.1 | 87.8 | 92.5 |
| | | | 0.0001 | 96.2 | 96.2 | 95.7 | 96.8 |
| | | 16 | 0.1 | 67.6 | 74.6 | 61.2 | 95.7 |
| | | | 0.01 | 81.9 | 82.6 | 79.4 | 86.1 |
| | | | 0.001 | 90.4 | 89.5 | 98.7 | 81.9 |
| | | | 0.0001 | 98.9 | 98.9 | 100 | 97.8 |
| | | 8 | 0.1 | 75 | 78.3 | 69.1 | 90.4 |
| | | | 0.01 | 89.4 | 88.2 | 98.6 | 79.7 |
| | | | 0.001 | 85.6 | 86 | 83.8 | 88.2 |
| | | | 0.0001 | 93.1 | 93.4 | 89.3 | 97.8 |
| | 70% | 32 | 0.1 | 76.1 | 71.6 | 87.7 | 60.5 |
| | | | 0.01 | 85.9 | 83.6 | 100 | 71.8 |
| | | | 0.001 | 92.3 | 91.9 | 95.4 | 88.7 |
| | | | 0.0001 | 98.6 | 98.6 | 97.2 | 100 |
| | | 16 | 0.1 | 59.2 | 30.9 | 100 | 18.3 |
| | | | 0.01 | 72.5 | 65.4 | 88 | 52.1 |
| | | | 0.001 | 95.1 | 94.8 | 98.4 | 91.5 |
| | | | 0.0001 | 98.6 | 98.6 | 98.6 | 98.6 |
| | | 8 | 0.1 | 59.9 | 37.3 | 85 | 23 |
| | | | 0.01 | 64.1 | 63.8 | 64.2 | 63.3 |
| | | | 0.001 | 62.7 | 47.5 | 80 | 33.8 |
| | | | 0.0001 | 99.3 | 99.2 | 100 | 98.5 |
| | 80% | 32 | 0.1 | 87.2 | 86.3 | 92.6 | 80.8 |
| | | | 0.01 | 73.4 | 69.1 | 82.2 | 59.5 |
| | | | 0.001 | 92.6 | 92.7 | 94.7 | 97.8 |
| | | | 0.0001 | 95.7 | 95.5 | 100 | 91.5 |
| | | 16 | 0.1 | 73.4 | 63.7 | 100 | 46.8 |
| | | | 0.01 | 62.8 | 49.2 | 77.2 | 36.1 |
| | | | 0.001 | 93.6 | 93.1 | 100 | 87.2 |
| | | | 0.0001 | 97.9 | 97.8 | 100 | 95.7 |
| | | 8 | 0.1 | 54.3 | 33.8 | 61.1 | 23.4 |
| | | | 0.01 | 77.7 | 71.2 | 100 | 55.3 |
| | | | 0.001 | 87.2 | 85.3 | 100 | 74.4 |
| | | | 0.0001 | 93.6 | 93.4 | 95.5 | 91.4 |

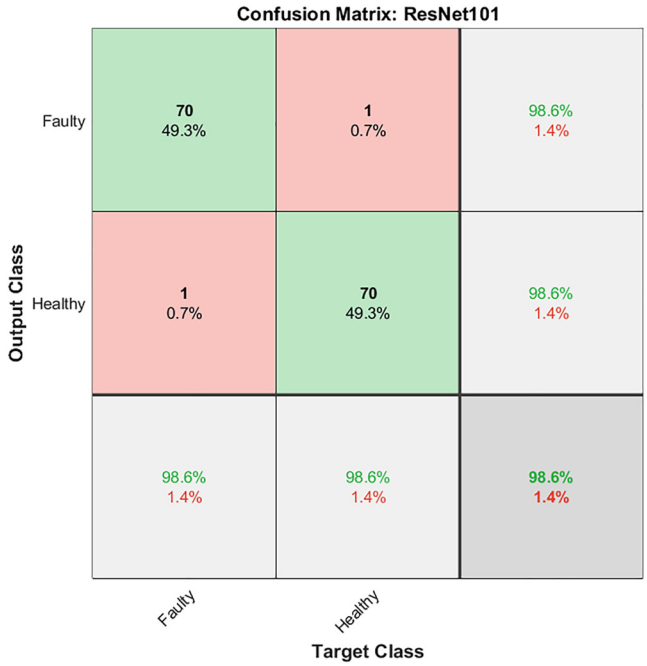


*Fig. 8.* Confusion matrix of ResNet 101

*Table 6.* Best results of all networks

| Net | Metrics | | | |
|---|---|---|---|---|
| | ACC | F1 Score | Recall | Precision |
| ResNet 18 | 98.9 | 98.9 | 100 | 97.8 |
| ResNet 50 | 100 | 100 | 100 | 100 |
| ResNet 101 | 98.6 | 98.6 | 98.6 | 98.6 |

## 5. CONCLUSION

This paper focused on developing an automated method to accurately classify the electrical faults that occur in the PMSM. The complexities of using the signals which require more processing techniques and more time for training the network, signal to image approach is applied. However, the purpose of the research was to look into ResNet's potential for maintenance planning. The experimental results demonstrated that ResNet 50 achieved accurate fault classification when trained from scratch on our data which is limited and complicated in structure, however, the network achieved the state-of-the-art of 100% accuracy, recall, precision, and F1 score respectively. The evaluation metrics also show that the proposed network results are enhanced when fine-tuning is applied.

In the future work, one may suggest that other types of pre-trained networks can be used and compared to the proposed method [19–24]. Furthermore, other kinds of motors will be considered and added to our data to create more variety in the dataset. One can extend this study to include various control schemes for the motor under consideration taking into account the faults deduced from this study to present a fault controlled for PMSM based on ResNet Neural Network [25–39].

## REFERENCES

[1] A. J. Humaidi and A. H. Hameed, "PMLSM position control based on continuous projection adaptive sliding mode controller," *Syst. Sci. Control Eng.*, vol. 6, no. 3, 2018. https://doi.org/10.1080/21642583.2018.1547887.

[2] B. Aubert, J. Régnier, S. Caux, and D. Alejo, "Kalman-filter-based indicator for online interturn short circuits detection in permanent-magnet synchronous generators," *IEEE Trans. Ind. Electron.*, vol. 62, no. 3, pp. 1921–30, March 2015. https://doi.org/10.1109/TIE.2014.2348934.

[3] Z. Gao, C. Cecati, and S. X. Ding, "A survey of fault diagnosis and fault-tolerant techniques—Part I: fault diagnosis with model-based and signal-based approaches," *IEEE Trans. Ind. Electron.*, vol. 62, no. 6, pp. 3757–67, June 2015. https://doi.org/10.1109/TIE.2015.2417501.

[4] X. Dai and Z. Gao, "From model, signal to knowledge: a data-driven perspective of fault detection and diagnosis," *IEEE Trans. Ind. Inform.*, vol. 9, no. 4, pp. 2226–38, Nov. 2013. https://doi.org/10.1109/TII.2013.2243743.

[5] C. G. Dias and F. H. Pereira, "Broken rotor bars detection in induction motors running at very low slip using a hall effect sensor," *IEEE Sensors J.*, vol. 18, no. 11, pp. 4602–13, 1 June, 2018. https://doi.org/10.1109/JSEN.2018.2827204.

[6] H. Liu, J. Zhou, Y. Xu, Y. Zheng, X. Peng, and W. Jiang, "Unsupervised fault diagnosis of rolling bearings using a deep neural network based on generative adversarial networks," *Neurocomputing*, vol. 315, pp. 412–24, Nov. 2018. https://doi.org/10.1016/j.neucom.2018.07.034.

[7] M. Altobi, G. Bevan, P. Wallace, D. Harrison, and K. Ramachandran, "Fault diagnosis of a centrifugal pump using MLP-GABP and SVM with CWT," *Eng. Sci. Technol. Int. J.*, vol. 22, no. 3, pp. 854–61, Jun. 2019. https://doi.org/10.1016/j.jestch.2019.01.005.

[8] S. Moosavi, A. Djerdir, Y. Amirat, and D. Khaburi, "ANN-based fault diagnosis of permanent magnet synchronous motor under stator winding shorted turn," *Electric Power Syst. Res.*, vol. 125, pp. 67–82, Aug. 2015. https://doi.org/10.1016/j.epsr.2015.03.024.

[9] W. Ahmad, S. A. Khan, and J.-M. Kim, "A hybrid prognostics technique for rolling element bearings using adaptive predictive models," *IEEE Trans. Ind. Electron.*, vol. 65, no. 2, pp. 1577–84, Feb. 2018. https://doi.org/10.1109/TIE.2017.2733487.

[10] W. Abed, Q. Aish, and A. Hamed, "Performance monitoring of aircraft PMSM based on soft computing technique," *Periodicals Eng. Nat. Sci. (Pen)*, vol. 9, no. 1, p. 293, 2021. https://doi.org/10.21533/pen.v9i1.1797.

[11] Y. Chen, S. Liang, W. Li, H. Liang, and C. Wang, "Faults and diagnosis methods of permanent magnet synchronous motors," *Appl. Sci.*, vol. 9, no. 10, p. 2116, May. 2019. https://doi.org/10.3390/app9102116.

[12] J. Sun, C. Yan, and J. Wen, "Intelligent bearing fault diagnosis method combining compressed data acquisition and deep learning," *IEEE Trans. Instrumentation Meas.*, vol. 67, no. 1, pp. 185–95, Jan. 2018. https://doi.org/10.1109/TIM.2017.2759418.

[13] Y. Lei, F. Jia, J. Lin, S. Xing, and S. X. Ding, "An intelligent fault diagnosis method using unsupervised feature learning towards mechanical big data," *IEEE Trans. Ind. Electron.*, vol. 63, no. 5, pp. 3137–47, May 2016. https://doi.org/10.1109/TIE.2016.2519325.

[14] T. Ince, S. Kiranyaz, L. Eren, M. Askar, and M. Gabbouj, "Real-time motor fault detection by 1-D convolutional neural networks," *IEEE Trans. Ind. Electron.*, vol. 63, no. 11, pp. 7067–75, Nov. 2016. https://doi.org/10.1109/TIE.2016.2582729.

[15] Z. Ullah, S.-T. Lee, and J. Hur, "A torque angle-based fault detection and identification technique for IPMSM," *IEEE Trans. Industry Appl.*, vol. 56, no. 1, pp. 170–82, Jan.-Feb. 2020. https://doi.org/10.1109/TIA.2019.2947401.

[16] C. Lu, Y. Wang, M. Ragulskis, and Y. Cheng, "Fault diagnosis for rotating machinery: a method based on image processing," *PLoS One*, Oct. 2016. https://doi.org/10.1371/journal.pone.0164111.

[17] E. Balaban, P. Bansal, P. Stoelting, A. Saxena, K. F. Goebel, and S. Curran, "A diagnostic approach for electro-mechanical actuators in aerospace systems," *2009 IEEE Aerospace Conference*, Big Sky, MT, USA, 2009, vol. 4, pp. 1–13, Feb. 2021. https://doi.org/10.1109/AERO.2009.4839661.

[18] M. Hussain, A. R. Rizwan, I. H. Kalwar, and D. T. Memon, "Multiple faults detection and identification of three phase induction motor using advanced signal processing techniques," *3C Tecnología, Spec. Issue*, pp. 93–117, Nov. 2020. https://doi.org/10.17993/3ctecno.2020.specialissue6.93-117.

[19] R. H. Hadi, H. N. Hady, A. M. Hasan, A. Al-Jodah, and A. J. Humaidi, "Improved Fault classification for predictive maintenance in industrial IoT based on AutoML: a case study of ball-bearing faults," *Processes*, vol. 11, no. 5, p. 1507, 2023. https://doi.org/10.3390/pr11051507.

[20] A. R. Ajel, A. Q. Al-Dujaili, Z. G. Hadi, and A. J. Humaidi, "Skin cancer classifier based on convolution residual neural network," *Int. J. Electr. Comput. Eng. (IJECE)*, vol. 13, no. 6, pp. 6240–8, 2023. https://doi.org/10.11591/ijece.v13i6.pp6240-6248.

[21] A. R. Nasser, A. M. Hasan, and A. J. Humaidi, "DL-AMDet: Deep learning-based malware detector for android," *Intell. Syst. Appl.*, vol. 21, no. 200318, pp. 1–10, 2024. https://doi.org/10.1016/j.iswa.2023.200318.

[22] J. Abdulhadi, A. Al-Dujaili, A. J. Humaidi, and M. A. R. Fadhel, "Human nail diseases classification based on transfer learning," *ICIC Express Lett.*, vol. 15, no. 12, pp. 1271–82, 2021.

[23] H. Al-Khazraji, A. R Nasser, A. M. Hasan, A. K. Al Mhdawi, H. Al-Raweshidy, and A. J. Humaidi, "Aircraft engines remaining useful life prediction based on A hybrid model of autoencoder and deep belief network," *IEEE Access*, vol. 10, pp. 82156–63, 2022. https://doi.org/10.1109/ACCESS.2022.3188681.

[24] M. Al-Amidie, A. Al-Asadi, A. J. Humaidi, A. Al-Dujaili, L. Alzubaidi, L. Farhan, M. A. Fadhel, R. G. McGarvey, and N. E. Islam, "Robust spectrum sensing detector based on MIMO cognitive radios with non-perfect channel gain," *Electronics*, vol. 10, p. 529, 2021. https://doi.org/10.3390/electronics10050529.

[25] A. Al-Dujaili, V. Cocquempot, M. E. B. E. Najjar, D. Pereira, and A. Humaidi, "Adaptive fault-tolerant control design for multi-linked two-wheel drive mobile robots. Mobile robot: Motion control and path planning," *1090, Springer International Publishing*, pp. 283–329, 2023. https://doi.org/10.1007/978-3-031-26564-8_10, Studies in Computational Intelligence.

[26] A. Q. Al-Dujaili, A. J. Humaidi, Z. T. Allawi, and M. E. Sadiq, "Earthquake hazard mitigation for uncertain building systems based on adaptive synergetic control," *Appl. Syst. Innovation*, vol. 6, no. 2, p. 34, 2023. https://doi.org/10.3390/asi6020034.

[27] A. F. Hasan, N. Al-Shamaa, S. S. Husain, A. J. Humaidi, and A. Al-dujaili, "Spotted hyena optimizer enhances the performance of fractional-order PD controller for tri-copter drone," *Int. Rev. Appl. Sci. Eng.*, vol. 15, no. 1, pp. 82–94, 2023. https://doi.org/10.1556/1848.2023.00659.

[28] A. Al-Dujaili, et al., "Fault diagnosis and Fault tolerant control for -linked two wheel drive mobile robots," in *Mobile Robot: Motion Control and Path Planning. Studies in Computational Intelligence*, vol. 1090, A. T. Azar, I. Kasim Ibraheem, and A. Jaleel Humaidi, Eds., Cham: Springer, 2023.

[29] A. K. Mohammed, N. K. Al-Shamaa, and A. Q. Al-Dujaili, "Super-Twisting sliding mode control of permanent magnet DC motor," in *2022 IEEE 18th International Colloquium on Signal Processing & Applications (CSPA)*, May 2022, pp. 347–52.

[30] A. K. Mohammed, A. Q. Al-Dujaili, and N. K. Al-Shamaa, "Real-time design and implementation of nonlinear speed controller for permanent magnet DC motor based on PSO tuner," in *2021 IEEE International Conference on Automatic Control & Intelligent Systems (I2CACIS)*, 2021, pp. 323–8.

[31] A. J. Humaidi and M. R. Hameed, "Development of a new adaptive backstepping control design for a non-strict and under-actuated system based on a PSO tuner," *Information (Switzerland)*, vol. 10, no. 2, supp. 38, pp. 1193–204, 2019. https://doi.org/10.3390/info10020038.

[32] A. J. Humaidi, M. R. Hameed, A. F. Hasan, A. S. M. Al-Obaidi, A. T. Azar, I. K. Ibraheem, A. Q. Al-Dujaili, A. K. Al Mhdawi, and F. A. Abdulmajeed, "Algorithmic design of block backstepping motion and stabilization control for segway mobile robot," in *Mobile Robot: Motion Control and Path Planning. Studies in Computational Intelligence*, vol. 1090, A. T. Azar, I. Kasim Ibraheem, and A. Jaleel Humaidi, Eds., Cham: Springer, 2023.

[33] A. F. Hasan, A. J. Humaidi, A. S. M. Al-Obaidi, A. T. Azar, I. K. Ibraheem, A. Q. Al-Dujaili, A. K. Al-Mhdawi, and F. A. Abdulmajeed, "Fractional order extended state observer enhances the performance of controlled tri-copter UAV based on active disturbance rejection control," in *Mobile Robot: Motion Control and Path Planning. Studies in Computational Intelligence*, vol. 1090, A. T. Azar, I. Kasim Ibraheem, and A. Jaleel Humaidi, Eds., Cham: Springer, 2023.

[34] S. S. Husain, A. Q. Al-Dujaili, A. A. Jaber, A. J. Humaidi, and R. S. Al-Azzawi, "Design of a robust controller based on barrier function for vehicle steer-by-wire systems," *World Electr. Veh. J.*, vol. 15, no. 1, supp. 17, 2024. https://doi.org/10.3390/wevj15010017.

[35] A. Hussein, A. T. Abdulameer, A. Abdulkarim, H. Husni, and D. Al-Ubaidi, "Classification of dyslexia among school students using deep learning," *J. Tech.*, vol. 6, no. 1, pp. 85–92, 2024. https://doi.org/10.51173/jt.v6i1.1893.

[36] M. Y. Hassan, A. J. Humaidi, and M. K. Hamza, "On the design of backstepping controller for Acrobot system based on adaptive observer," *Int. Rev. Electr. Eng.*, vol. 15, no. 4, pp. 328–35, 2020. https://doi.org/10.15866/iree.v15i4.17827.

[37] A. T. Mohammad and J. Parchami, "Improving diabetic patients monitoring system using (NCA-CNN) algorithm based on loT,"

*J. Tech.*, vol. 6, no. 2, pp. 9–17, 2024. https://doi.org/10.51173/jt.v6i2.2316.

[38] A. J. Humaidi and M. R. Hameed, "Design and performance investigation of block-backstepping algorithms for ball and arc system," in *IEEE International Conference on Power, Control, Signals and Instrumentation Engineering, ICPCSI 2017*, 2018, pp. 325–32. https://doi.org/10.1109/ICPCSI.2017.8392309.

[39] S. A. AL-Hashemi, A. AL-Dujaili, and A. R. Ajel, "Speed control using an integral sliding mode controller for a three-phase induction motor," *J. Tech.*, vol. 3, no. 3, pp. 10–9, 2021. https://doi.org/10.51173/jt.v3i3.328.